⌘ *Author's Choice*

THE JOURNAL OF BIOLOGICAL CHEMISTRY VOL. 287, NO. 16, pp. 12952–12965, April 13, 2012

Identification and Profiling of Novel α_{1A}-Adrenoceptor-CXC Chemokine Receptor 2 Heteromer*[S]

Received for publication, November 10, 2011, and in revised form, February 20, 2012 Published, JBC Papers in Press, February 27, 2012, DOI 10.1074/jbc.M111.322834

Sanam Mustafa[‡1], Heng B. See[‡1], Ruth M. Seeber[‡], Stephen P. Armstrong[‡], Carl W. White[§], Sabatino Ventura[§], Mohammed Akli Ayoub[‡], and Kevin D. G. Pfleger[‡¶2]

From the [‡]Laboratory for Molecular Endocrinology-G Protein-Coupled Receptors, Western Australian Institute for Medical Research and Centre for Medical Research, The University of Western Australia, Nedlands, Perth, Western Australia 6009, [§]Drug Discovery Biology, Monash Institute of Pharmaceutical Sciences, Monash University, Parkville, Victoria 3052 and [¶]Dimerix Bioscience Pty Ltd, Nedlands, Perth, Western Australia 6009, Australia

Background: Receptor heteromers are macromolecular complexes containing at least two different receptor subunits, resulting in distinct pharmacology.
Results: The observed α_{1A}AR-CXCR2 heteromer recruits β-arrestin strongly upon activation with norepinephrine, in contrast to α_{1A}AR alone.
Conclusion: Heteromerization with CXCR2 dramatically changes α_{1A}AR pharmacology, revealing the potential for heteromer-specific biased agonism.
Significance: Such heteromer-specific novel pharmacology has important implications for drug discovery.

We have provided the first evidence for specific heteromerization between the α_{1A}-adrenoceptor (α_{1A}AR) and CXC chemokine receptor 2 (CXCR2) in live cells. α_{1A}AR and CXCR2 are both expressed in areas such as the stromal smooth muscle layer of the prostate. By utilizing the G protein-coupled receptor (GPCR) heteromer identification technology on the live cell-based bioluminescence resonance energy transfer (BRET) assay platform, our studies in human embryonic kidney 293 cells have identified norepinephrine-dependent β-arrestin recruitment that was in turn dependent upon co-expression of α_{1A}AR with CXCR2. These findings have been supported by co-localization observed using confocal microscopy. This norepinephrine-dependent β-arrestin recruitment was inhibited not only by the α_1AR antagonist Terazosin but also by the CXCR2-specific allosteric inverse agonist SB265610. Furthermore, Labetalol, which is marketed for hypertension as a nonselective β-adrenoceptor antagonist with α_1AR antagonist properties, was identified as a heteromer-specific-biased agonist exhibiting partial agonism for inositol phosphate production but essentially full agonism for β-arrestin recruitment at the α_{1A}AR-CXCR2 heteromer. Finally, bioluminescence resonance energy transfer studies with both receptors tagged suggest that α_{1A}AR-CXCR2 heteromerization occurs constitutively and is not modulated by ligand. These findings support the concept of GPCR heteromer complexes exhibiting distinct pharmacology, thereby providing additional mechanisms through which GPCRs can potentially achieve their diverse biological functions. This has important implications for the use and future development of pharmaceuticals targeting these receptors.

G protein-coupled receptors (GPCRs)[3] are expressed in almost every human cell and have diverse physiological and pathophysiological roles. Our understanding of GPCR signaling is now evolving from considering these seven transmembrane receptors (7TMRs) simply as "on-off" switches consisting of only one functional unit to accepting that they probably act more like "microprocessors" (1), signaling complexes containing potentially multiple GPCRs along with various other interacting proteins. Termed heteromerization, the accepted definition states that a receptor heteromer is a "macromolecular complex composed of at least two (functional) receptor units with biochemical properties that are demonstrably different from those of its individual components" (2). Recent evidence has suggested that GPCRs can function as monomers (3–6) as well as forming complexes containing only one type of GPCR (termed "homomers" (2)). Consequently, for most GPCRs, heteromerization is probably not obligatory. However, it does have the potential to provide additional mechanisms for signal integration and allosteric modulation when it occurs, and with these come exciting new opportunities for novel pharmaceutical development.

The α_{1A}AR is coupled to the $G_{q/11}$ protein/phospholipase C signaling pathway. Subsequent activation of phospholipase C

* This research was funded by National Health and Medical Research Council of Australia Project Grant 566736 and Dimerix Bioscience Pty Ltd. K. D. G. P. is an Australian Research Council Future Fellow (FT100100271) as well as Chief Scientific Officer of Dimerix Bioscience Pty Ltd, a spin-out company of the University of Western Australia that has been assigned the rights to the GPCR-HIT technology. K. D. G. P. has a minor shareholding in Dimerix.
⌘ *Author's Choice*—Final version full access.
[S] This article contains supplemental Figs. 1–3.
[1] Both authors contributed equally to this work.
[2] To whom correspondence should be addressed: Western Australian Institute for Medical Research, B Block, QEII Medical Centre, Nedlands, Perth, Western Australia 6009, Australia. Tel.: 618-9346-1980; Fax: 618-9346-1818; E-mail: kevin.pfleger@waimr.uwa.edu.au.

[3] The abbreviations used are: GPCR, G protein-coupled receptor; HIT, heteromer identification technology; α_{1A}AR, α_{1A}-adrenoceptor; AR, adrenoceptor; BRET, bioluminescence resonance energy transfer; eBRET, extended BRET; HEK, human embryonic kidney; NE, norepinephrine; OxR1, orexin receptor 1; Rluc, *Renilla* luciferase; RT, room temperature; V2R, vasopressin receptor 2; CXCR2, CXC chemokine receptor 2; GLP-1, glucagon-like peptide-1.

causes the production of inositol trisphosphate and diacylglycerol, particularly resulting in contraction of smooth muscle (7).

Currently, α_{1A}ARs can be functionally subclassified into two pharmacologically distinct phenotypes; the "standard" α_{1A}AR phenotype is predominantly found in brain, heart, and blood vessels, whereas a functional isoform of α_{1A}AR, the so-called "α_{1L}AR," is more prominent in prostate and bladder neck (8, 9). Using genetically modified knock-out mice, it has recently been shown that both functional phenotypes arise from the same α_{1A}AR gene (10) even though studies have indicated that a splice variant or polymorphism is not responsible for the difference in pharmacology (11–13). Furthermore, the α_{1L}AR phenotype is not observed in radioligand binding experiments using homogenized prostate tissue but is seen in functional studies using whole tissue or cells (14, 15). This has led to the suggestion that an interacting protein may be associated with the α_{1A}AR in tissues exhibiting α_{1L}AR pharmacology (14, 15). Indeed, a recent publication has provided evidence for cysteine-rich with epidermal growth factor-like domain 1α (CRELD1α) interacting with α_{1A}AR to modulate function, largely in terms of receptor expression levels (16). Evidence for α_{1A}AR forming complexes with itself (13, 17), with splice variants (13), and with α_{1B}AR (17) has also been published. No effects on receptor pharmacological properties were observed, but co-expression of α_{1B}AR did appear to increase α_{1A}AR expression levels (17).

Our hypothesis is that α_{1A}AR function can also be modulated by heteromerization with GPCRs from outside the adrenoceptor family. Interestingly, in addition to the aforementioned precedents for α_{1A}AR being modulated by interacting proteins, recent evidence for heteromerization of the β2-adrenoceptor (β_2AR) and CXC chemokine receptor 4 playing a potential role in cardiac myocyte survival has provided a precedent for adrenoceptor-chemokine receptor heteromerization (18). Taken together with suggestions that the diverse functional effects mediated by the α_1ARs may not be entirely explicable by $G_{q/11}$ signaling pathways (19), we hypothesize that heteromerization may provide a mechanism for such diversity. This in turn provides a potential opportunity to develop therapies that target this receptor only when in a complex with another GPCR and, therefore, possibly also in a tissue-selective manner.

Although the chemokine receptors clearly play a major role in the immune system, their widespread expression pattern suggests their role may extend beyond chemotaxis and cell migration. CXCR2 is activated by multiple chemokines, and signaling via this receptor has been shown to reinforce cell growth arrest (cellular senescence) (20). In contrast, depletion of CXCR2 results in escape from senescence. A role for CXCR2 in senescence has been elucidated in prostate intraepithelial neoplasia, with fibroblasts that are undergoing oncogene-induced senescence up-regulating CXCR2 and its ligands, suggestive of a positive feedback loop (20). Furthermore, CXCR2 is well established as a receptor that is capable of forming complexes with both itself (21, 22) and other GPCRs (22, 23).

Although establishment of novel heteromer-specific pharmacology in native tissue is the ultimate goal, this is hampered by the general lack of experimental tools to study heteromerization of endogenously expressed receptors (24). Therefore, our first step has been to provide evidence at least of receptor co-localization, which we have done using immunohistochemistry that indicates CXCR2 expression specifically in a region of the prostate well established as expressing α_{1A}AR (25). Our next step has been to establish the existence and novel pharmacology of α_{1A}AR heteromerization in a recombinant system, to identify the "biochemical fingerprint of a receptor heteromer." By applying the GPCR heteromer identification technology (HIT) approach (24, 26–29) on a live cell bioluminescence resonance energy transfer (BRET) platform, supported by confocal microscopy experiments, we have provided evidence for novel and specific heteromerization between α_{1A}AR and CXCR2 that results in norepinephrine (NE)-induced recruitment of β-arrestin2 to the receptor complex. This is in stark contrast to the very weak β-arrestin2 interaction observed with α_{1A}AR monomers/homomers in transfected HEK293 cells (30) but, very interestingly, is consistent with the observation of α_{1A}AR·β-arrestin2 complex formation specifically in prostate stroma (31).

EXPERIMENTAL PROCEDURES

Materials—α_{1A}AR and CCR2 cDNAs were obtained from the Missouri S&T cDNA Resource Center. CXCR2 cDNA was kindly provided by Aron Chakera (Oxford University). CCR2/Rluc8 and CXCR2/Rluc8 cDNA constructs were generated from plasmids containing the respective receptor cDNA tagged with *Renilla* luciferase (Rluc), also kindly provided by Aron Chakera. Similarly, the α_{1A}AR/Rluc8 and orexin receptor 1 (OxR1)/Rluc8 cDNA constructs were generated from α_{1A}AR/Rluc and OxR1/Rluc, respectively (formerly produced by PCR amplification of receptor cDNA to remove the stop codon and ligation into pcDNA3 containing Rluc). OxR1/Rluc was generated previously in our laboratory by Matthew Dalrymple from OxR1 cDNA kindly provided by Masashi Yanagisawa (Howard Hughes Medical Institute). With all of these constructs, the Rluc coding region was replaced with Rluc8 cDNA from pcDNA3.1-Rluc8 kindly provided by Andreas Loening and Sanjiv Gambhir (Stanford University) (32) as described previously for other GPCR constructs (33). Vasopressin receptor 2 (V2R)/Rluc8 was generated as described previously from V2R cDNA kindly provided by Brian Feldman (Stanford University) (34). The β-arrestin2/Venus cDNA construct was prepared previously from pcC2-Venus kindly provided by Atsushi Miyawaki (RIKEN Brain Science Institute, Wako-city, Japan) (33). CXCR2/Venus and V2R/Venus were prepared by replacing Rluc8 cDNA with Venus cDNA in the CXCR2/Rluc8 and V2R/Rluc8 constructs, respectively, as described previously for V2R/Venus (34). Ligands used were NE, CXCL8 (Interleukin-8), CCL2 (MCP-1), arginine vasopressin, Terazosin, and Labetalol (Sigma) as well as SB265610 (Tocris) and Orexin A (American Peptide Co.).

Cell Culture and Transfection—HEK293FT cells were maintained at 37 °C in 5% CO_2 and complete media (Dulbecco's modified Eagle's medium (DMEM) containing 0.3 mg/ml glutamine, 100 IU/ml penicillin and 100 μg/ml streptomycin (Invitrogen)) supplemented with 10% fetal calf serum (FCS) and 400 μg/ml Geneticin (Invitrogen). Transient transfections were carried out 24 h after seeding about 550,000 cells/well of a

6-well plate. Genejuice (Novagen) transfection reagent was used according to the manufacturer's instructions. Cells were harvested with 0.05% trypsin-EDTA (Invitrogen). For testing the CXCR2 antibody specificity, Chinese hamster ovary (CHO) cells were seeded at a density of 40,000 cells/well of a 12-well plate and transiently transfected using Lipofectamine (Invitrogen) as per the manufacturer's instructions. Cells were maintained at 37 °C in 5% CO_2 and high glucose (25 mM) DMEM (supplemented with 4 mM Glutamax (Invitrogen), 5% FCS, 16 mM HEPES, 100 IU/ml penicillin, 100 μg/ml streptomycin, 1 mg/ml hygromycin B, and 1 mM sodium pyruvate).

Assessment of CXCR2 Antibody Specificity—CHO cells were immunostained 36 h after transfecting with 1 μg of CXCR2 or CCR2 cDNA per well of a 12-well plate. Cells were washed with phosphate-buffered saline (PBS) and fixed with 4% paraformaldehyde in PBS for 10 min at room temperature (RT). After three 10-min washes in PBS, the cells were blocked and permeabilized (30 min, RT) with 5% donkey serum in PBS containing 0.1% Triton X-100 and incubated overnight at 4 °C with rabbit polyclonal anti-CXCR2 antibodies (1:200; Abcam, ab14935) in PBS containing 5% donkey serum, 0.1% sodium azide, and 0.1% Triton X-100. Cells were then washed as above and incubated with Alexa Fluor 594 donkey anti-rabbit antibodies (1:200; Invitrogen; 1 h, RT). Cells were washed again as above, and the nucleus was stained with TO-PRO-3 Iodide (1:3000 in PBS, Invitrogen). Images were acquired using a Nikon A1R confocal microscope with 561 and 640 lasers and 595/50 and 700/75 emission filters, respectively, as well as a Nikon S Plan Fluor 40× objective lens. 12 bit (1024 × 1024) images were collected using the NIS Elements software.

Prostate Immunohistochemistry—Male C57Bl6/J mice were killed by cervical dislocation, and the ventral prostate was dissected out. Tissue was fixed in 4% formaldehyde in PBS (2 h, RT), washed 4 times with 7% sucrose in PBS containing 0.01% sodium azide (10 min each time), and stored in this solution (48 h, 4 °C). Prostates were then embedded in optimum cutting temperature compound (Sakura Finetek), snap-frozen in melting isopentane, and stored at −80 °C until use. Frozen 10-μm prostate sections were cut using a cryostat (Leica CM 1850), thawed onto Superfrost Plus slides (Menzel-Glaser), and left to air dry (1 h). Sections were washed with PBS (10 min) then blocked with 10% donkey serum and 1% bovine serum albumin (BSA) in PBS containing 0.1% lysine, 0.1% sodium azide, and 0.2% Tween 20 (30 min, RT). After blocking, slide-mounted sections were incubated (40–48 h, 4 °C) with rabbit polyclonal anti-CXCR2 antibodies (1:100; Abcam, ab14935) in PBS containing 0.01% BSA, 5% donkey serum, 0.1% lysine, 0.1% sodium azide, and 0.1% Tween 20. For negative control sections, rabbit polyclonal anti-CXCR2 antibodies were omitted. Sections were washed 4 times with PBS (10 min each time) and incubated with fluorescein isothiocyanate (FITC)-conjugated donkey anti-rabbit antibodies (1:200; Jackson ImmunoResearch Laboratories; 1 h, RT). After secondary antibody incubation, sections were again washed 4 times with PBS (10 min each time), then stained (10 min, RT) with DAPI (300 ng/ml, Sigma) in PBS. Sections were then washed with PBS and mounted with Vectashield mounting media (Vector Laboratories). Sections were viewed using an Olympus BX61 fluorescence microscope fitted with an Olympus mercury burner light source attachment and Olympus UPlanSApo 20× and 40× objectives. CXCR2 staining (FITC, *green*) was viewed using an Olympus U-MNIBA3 filter cube consisting of a DM505 dichroic mirror, BP470-490 exciter filter, and BA515-550 barrier filter. Staining for DAPI (blue) was viewed using an Olympus U-MNUA2 filter cube consisting of a DM400 dichroic mirror, BP360-370 exciter filter, and BA420-460 barrier filter. An Olympus F-view II digital camera and analySIS LS Research software were used to acquire 16 bit photomicrographs. Prior approval for animal experimentation was granted by the Monash University Standing Committee on Animal Ethics (VCPA 2009/15).

GPCR-HIT BRET Assays—As described previously (27), HEK293FT cells were transiently transfected with cDNA encoding a GPCR fused to Rluc8 (GPCR/Rluc8) and β-arrestin2 fused to Venus (β-arrestin2/Venus) along with a second GPCR that was untagged with respect to BRET signaling or empty vector. Initially DNA amounts of 0.7, 0.3, and 0.1 μg/well of a 6-well plate were used for each construct respectively, but this was changed to 0.1, 0.3, and 0.1 μg/well, respectively, after extensive cDNA titration assays (supplemental Fig. 1). 48 h post-transfection cells were incubated at 37 °C, 5% CO_2 for 2 h with 30 μM EnduRen (Promega) to ensure substrate equilibrium was reached. BRET measurements were taken at 37 °C using the VICTOR Light plate reader with Wallac 1420 software (PerkinElmer Life Sciences). Filtered light emissions were sequentially measured at 400–475 and 520–540 nm. The BRET signal was calculated by subtracting the ratio of 520–540 nm emission over 400–475-nm emission for a vehicle-treated cell sample from the same ratio for a second aliquot of the same cells treated with agonist, as described previously (35, 36). In this calculation the vehicle-treated cell sample represents the background, eliminating the requirement for measuring a donor-only control sample (35, 36). For these BRET kinetic assays, the final pretreatment reading is presented at the zero time point (time of ligand/vehicle addition). The situation where the addition of ligand specific for the untagged GPCR results in a ligand-induced BRET signal indicates β-arrestin binding specifically to a heteromer complex (27).

Measurement of Fluorescence—Fluorescence after light excitation was measured on an EnVision 2102 multilabel plate reader (PerkinElmer Life Sciences) using a 485/14 excitation filter, 535/25 emission filter, and D505 mirror.

BRET Assays with Both Receptors Tagged—BRET saturation assays were performed using HEK293FT cells transiently transfected with cDNA encoding α_{1A}AR/Rluc8 and either CXCR2/Venus, V2R/Venus, or pcDNA3 empty vector only, the latter being donor-only control cells. 0.05 μg of α_{1A}AR/Rluc8 cDNA along with between 0.01 and 0.85 μg of Venus-tagged receptor cDNA was transfected per well of a 6-well plate. In each case total cDNA was made up to 0.9 μg with pcDNA3 empty vector cDNA. For assessing the effect of ligands on the BRET between tagged receptors, cells were similarly transfected with cDNA encoding α_{1A}AR/Rluc8 and either CXCR2/Venus or pcDNA3 empty vector. 0.25 μg of each construct was transfected per well of a 6-well plate (0.5 μg/well total). Triplicate wells of each transfection were aliquoted into both a white well microplate for BRET measurements and a parallel black microplate for

fluorescence measurements. 48 h post-transfection, cells for BRET measurements were incubated at 37 °C, 5% CO_2 for 2 h with 30 μM EnduRen (Promega). Meanwhile, fluorescence measurements were taken after light excitation as described above. BRET measurements were taken at 37 °C using the VICTOR Light plate reader with Wallac 1420 software (PerkinElmer Life Sciences). Filtered light emissions were sequentially measured at 400–475 and 520–540 nm. The BRET ratio was calculated by subtracting the ratio of 520–540 nm emission over 400–475 nm emission for donor-only control cells from the same ratio for cells transfected with both α_{1A}AR/Rluc8 and Venus-tagged receptor, as described previously (35). The fluorescence/luminescence ratio for the BRET saturation assays was generated by dividing the fluorescence values in arbitrary units (obtained in parallel after laser excitation) by the luminescence values also in arbitrary units (obtained as part of the BRET assay).

Measurement of Total Inositol Phosphate Production Using [^{3}H]myo-Inositol—HEK293FT cells were seeded in 6-well plates and transiently transfected the next day. 24 h post-transfection cells were split into 24-well plates in inositol-free Complete Medium (MP Biomedicals) containing 1% dialyzed FCS. 6–8 h later medium was replaced with inositol-free medium containing 1% dialyzed FCS and 1 μCi/ml [^{3}H]*myo*-inositol (Amersham Biosciences) followed by overnight incubation. Total inositol phosphate production was then measured as described previously (35). This method was used to generate the data for Fig. 2*B*.

Measurement of Inositol 1-Phosphate Production Using Time-resolved FRET—The determination of inositol 1-phosphate accumulation was performed in 96-well microplates using the IP-One HTRF assay (CisBio Bioassays, Bagnol sur Ceze, France) (37). For most assays, cells were incubated for 1 h at 37 °C in the stimulation buffer (10 mM HEPES (pH 7.4), 1 mM $CaCl_2$, 0.5 mM $MgCl_2$, 4 mM KCl, 146 mM NaCl, 5.5 mM glucose, and 50 mM LiCl) with or without the indicated ligands. For the dose-response curves, cells were incubated in the stimulation buffer with NE or Labetalol at increasing doses for 40 min after preincubation with 10 μM Labetalol or vehicle for 20 min. Cells were then lysed using the conjugate-lysis buffer mixed with the terbium cryptate-labeled anti-inositol 1-phosphate antibody and the d2-labeled inositol 1-phosphate analog according to the manufacturer's instructions. The assay was incubated for 1 h at RT and terbium cryptate fluorescence and time-resolved FRET signal were measured at 620 and 665 nm, respectively, 50 μs after excitation at 337 nm using the PHERAstar FS (BMG Labtech, Mornington, Victoria, Australia) or EnVision 2102 (PerkinElmer Life Sciences) multilabel plate reader. This method was used to generate the data for Figs. 5*F*, 7, and 8, *B* and *D*.

Confocal Microscopy Assessing Localization—550,000 HEK293FT cells/well were seeded in a 6-well plate and transiently transfected the next day with 0.1 μg of HA-α_{1A}AR, 0.3 μg of β-arrestin2/Venus, and 0.1 μg of CXCR2 cDNA. Alternatively, cells were transfected with 0.3 μg of β-arrestin2/Venus cDNA with or without 0.1 μg of CXCR2 cDNA as controls. In each case total cDNA was made up to 0.5 μg with pcDNA3 empty vector cDNA. These cells were then seeded in 12-well plates containing sterile poly-D-lysine-coated coverslips at a density of 550,000 cells/well 24 h post-transfection and allowed to attach overnight at 37 °C in 5% CO_2. Treatments were carried out the next day; transfected cells were labeled with an anti-HA antibody (Sigma; 40 min) followed by ligand/vehicle treatment (30 min), both at 37 °C. Cells were washed with PBS at 4 °C and fixed with 4% (w/v) paraformaldehyde/5% (w/v) sucrose (10 min, RT) and washed again. Nuclei were stained with Hoechst 33258 (Invitrogen; 10 min, RT), and cells were permeabilized with 3% (w/v) milk, 0.15% (v/v) Triton X-100 (10 min, RT). Cells were then incubated with goat anti-rabbit Alexa 546 (Invitrogen; 1 h, RT). Cells were washed as before, and the coverslips mounted onto microscope slides with polyvinyl alcohol/glycerol mounting media. Coverslips were then sealed and stored at 4 °C in the dark until required. Cells were imaged with a Nikon A1Si confocal microscope with 405-, 488-, and 561-nm lasers utilizing a Nikon Apo 60×, NA 1.49 TIRF oil immersion lens. 12 bit, 1024 × 1024 pixel images were collected as Z-stacks with 4-line averaging and deconvoluted using the 3D Iterative Blind Deconvolution algorithm in the Lab Imaging package of NIS Elements software (Nikon).

Data Presentation and Statistical Analysis—Data were analyzed using Prism 5 graphing software (GraphPad) with α designated as 0.05. Sigmoidal curves were fitted to the dose-response data using non-linear regression. Statistical analysis of $\log EC_{50}$ values was carried out using one-way analysis of variance. BRET saturation curves were generated using non-linear regression assuming one site binding.

RESULTS

Prostate Immunohistochemistry—To assess CXCR2 expression in the prostate, we utilized an antibody that has been used extensively to label this receptor (38–41). This antibody labeled CXCR2-transfected CHO cells (supplemental Fig. 2*A*) but not CCR2-transfected (supplemental Fig. 2*B*) or mock-transfected (supplemental Fig. 2*C*) CHO cells assessed in parallel. Consequently, specific expression of CXCR2 was identified in the thin stromal smooth muscle layer of mouse prostate tissue (Fig. 1). Expression of α_{1A}AR in the prostate stroma is well established in the literature (42). Indeed, in the human prostatic α_{1A}ARs resulting in the α_{1L}AR phenotype are found exclusively in the stromal layer (25). Given this overlapping expression pattern in prostate tissue, specifically in prostate stroma, the functional interaction between α_{1A}AR and CXCR2 was further investigated in a recombinant system.

Profiling of Functional Interaction between α_{1A}AR and CXCR2—A very strong dose-dependent BRET signal, indicative of an α_{1A}AR-CXCR2 heteromer, was observed after NE treatment of HEK293FT cells expressing β-arrestin2/Venus, CXCR2/Rluc8, and untagged α_{1A}AR (Fig. 2*A*). This result was despite a distinct lack of BRET signal at any dose of NE with cells expressing β-arrestin2/Venus and α_{1A}AR/Rluc8 (Fig. 2*A*), consistent with previous evidence for α_{1A}AR interacting extremely weakly with β-arrestin in transfected HEK293 cells (30). The fusion with Rluc8 had no effect on NE-induced inositol phosphate signaling from the α_{1A}AR (Fig. 2*B*), providing evidence for the functionality of the α_{1A}AR/Rluc8 construct. Furthermore, co-expression of CXCR2 did not appear to influ-

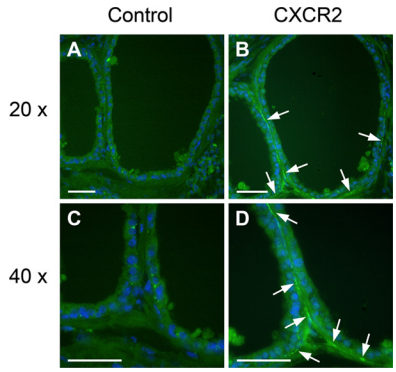

FIGURE 1. **Immunofluorescent localization of CXCR2 in the mouse prostate stroma.** Representative photomicrographs are shown ($n = 5$) of fixed, frozen cross-sections of the mouse prostate immunostained with rabbit polyclonal antibodies to CXCR2 (*green*) with DAPI (*blue*) counterstaining. The control section incubated without CXCR2 antibodies being present shows an absence of specific staining (*A*). In contrast, positive CXCR2 immunostaining can be seen specifically in the stroma, as indicated by *white arrows* (*B*). *Panels C* and *D* (40× objective) are higher magnification of *panels A* and *B* (20× objective), respectively. *Scale bars*, 50 μm.

ence NE-induced coupling to the inositol phosphate signaling pathway (Fig. 2*B*). The NE-induced BRET signal between CXCR2/Rluc8 and β-arrestin2/Venus was dependent upon the co-expression of α_{1A}AR, although α_{1A}AR was not required for strong CXCL8 (interleukin-8)-induced recruitment of β-arrestin2/Venus to CXCR2/Rluc8 (Fig. 2*C*). Although the signal obtained after co-stimulation with NE and CXCL8 was greater, it was clearly less than the sum of separate NE and CXCL8 treatments (Fig. 2*C*). BRET kinetic profiles for the reciprocal arrangement of α_{1A}AR/Rluc8 and β-arrestin2/Venus with or without CXCR2 were notably of much smaller magnitude (Fig. 2*D*), indicating substantially less resonance energy transfer. These profiles confirmed that both the NE- and CXCL8-induced BRET signals require the presence of CXCR2 and that NE induces little or no proximity between α_{1A}AR/Rluc8 and β-arrestin2/Venus in the absence of CXCR2 (Fig. 2*D*). Furthermore, co-treatment with both agonists results in a substantially greater signal with this orientation. These observations are consistent with CXCR2 playing a key role in the interaction of the heteromer with β-arrestin2.

BRET Titration Assays—Extensive titration assays were carried out to show the effect of varying the concentration and ratio of CXCR2/Rluc8, β-arrestin2/Venus, and α_{1A}AR cDNA transfected (supplemental Fig. 1). These experiments showed that specific ligand-induced BRET signals were obtained with a wide range of cDNA concentrations and ratios. Furthermore, these signals were similar when CXCL8-induced (supplemental Fig. 1, *A*, *B*, *E*, *F*, and *I*) compared with when NE-induced (supplemental Fig. 1, *C*, *D*, *G*, *H*, and *J*). Both CXCL8-induced (supplemental Fig. 1*F*) and NE-induced (supplemental Fig. 1*H*) BRET signals were obtained with very low concentrations of cDNA, providing further support for these signals not being artifacts of protein overexpression. Finally, when the donor cDNA amount was kept constant and acceptor cDNA amount increased, signal saturation was observed (supplemental Fig. 1, *I* and *J*), again providing evidence for signal specificity.

Confocal Microscopy Assessing Localization—To further support our findings, agonist-treated HEK293FT cells co-expressing HA-α_{1A}AR and β-arrestin2/Venus with or without untagged CXCR2 were visualized (Fig. 3). In the absence of ligand treatment, β-arrestin2/Venus was diffuse throughout the cytoplasm (Fig. 3, *F* and *H*), and HA-α_{1A}AR was primarily localized to the plasma membrane (Fig. 3, *K* and *M*) of both cell populations. This is particularly clear in the merged images (Fig. 3, *P* and *R*). NE treatment did not change this expression pattern in the absence of CXCR2 (Fig. 3, *G*, *L*, and *Q*). As mentioned previously, α_{1A}AR has been shown to interact very weakly, if at all, with β-arrestin2 (30); therefore, it is not surprising that NE treatment did not result in a change in the localization of β-arrestin2/Venus or noticeable α_{1A}AR internalization. However, in the presence of CXCR2, NE-induced HA-α_{1A}AR internalization into punctate vesicles was observed (Fig. 3*N*) along with some β-arrestin2/Venus translocation (Fig. 3*I*). CXCL8 treatment of cells expressing both receptors also resulted in β-arrestin2/Venus translocation (Fig. 3*J*) and HA-α_{1A}AR internalization (Fig. 3*O*), with colocalization of β-arrestin2/Venus and HA-α_{1A}AR clearly evident (Fig. 3*T*). These observations are consistent with the BRET data shown in Fig. 2 and support the role of CXCR2 in α_{1A}AR internalization.

Further controls are provided in the form of cells assessed in parallel that were transfected with β-arrestin2/Venus only or β-arrestin2/Venus and untagged CXCR2 in the absence of HA-α_{1A}AR (supplemental Fig. 3). No translocation was observed in β-arrestin2/Venus-transfected cells upon treatment with vehicle (supplemental Fig. 3*A*), NE (supplemental Fig. 3*B*), or CXCL8 (supplemental Fig. 3*C*). Similarly, no β-arrestin translocation was observed in cells transfected with β-arrestin2/Venus and CXCR2 upon treatment with vehicle (supplemental Fig. 3*D*) or NE (supplemental Fig. 3*E*); however, a punctate distribution was observed upon treatment with CXCL8 (supplemental Fig. 3*F*).

Use of Selective Inhibitors to Interrogate β-Arrestin2 Recruitment to Heteromer—Terazosin is a selective α_1AR antagonist (43), and SB265610 has recently been characterized as a cell-permeable selective allosteric inverse agonist of CXCR2 believed to bind to the intracellular C-terminal tail (44, 45).

With cells co-expressing CXCR2/Rluc8, β-arrestin2/Venus, and α_{1A}AR, as expected, Terazosin did not inhibit the CXCL8-induced BRET signal (Fig. 4*A*), but did inhibit the NE-induced BRET signal (Fig. 4*B*). Whether the former result indicates that CXCL8-induced β-arrestin recruitment to the α_{1A}AR-CXCR2 heteromer can occur in the presence of an α_1AR antagonist, or whether this BRET signal is predominantly from β-arrestin2/Venus recruitment to CXCR2/Rluc8 monomers/homomers is unclear. This ambiguity illustrates the value of profiling with the ligand specific for the untagged receptor. However, the data clearly demonstrate that NE-induced β-arrestin2 recruitment to the α_{1A}AR-CXCR2 heteromer requires the activation of α_{1A}AR.

A particularly important finding was that, in addition to blocking the CXCL8-induced BRET signal (Fig. 4*A*), SB265610 also blocked the NE-induced BRET signal about as effectively as terazosin (Fig. 4*B*). Terazosin and SB265610 in combination had the same effect on blocking CXCL8-induced BRET as SB265610 alone (Fig. 4*A*), whereas the combination had a slightly greater effect on blocking NE-induced BRET compared

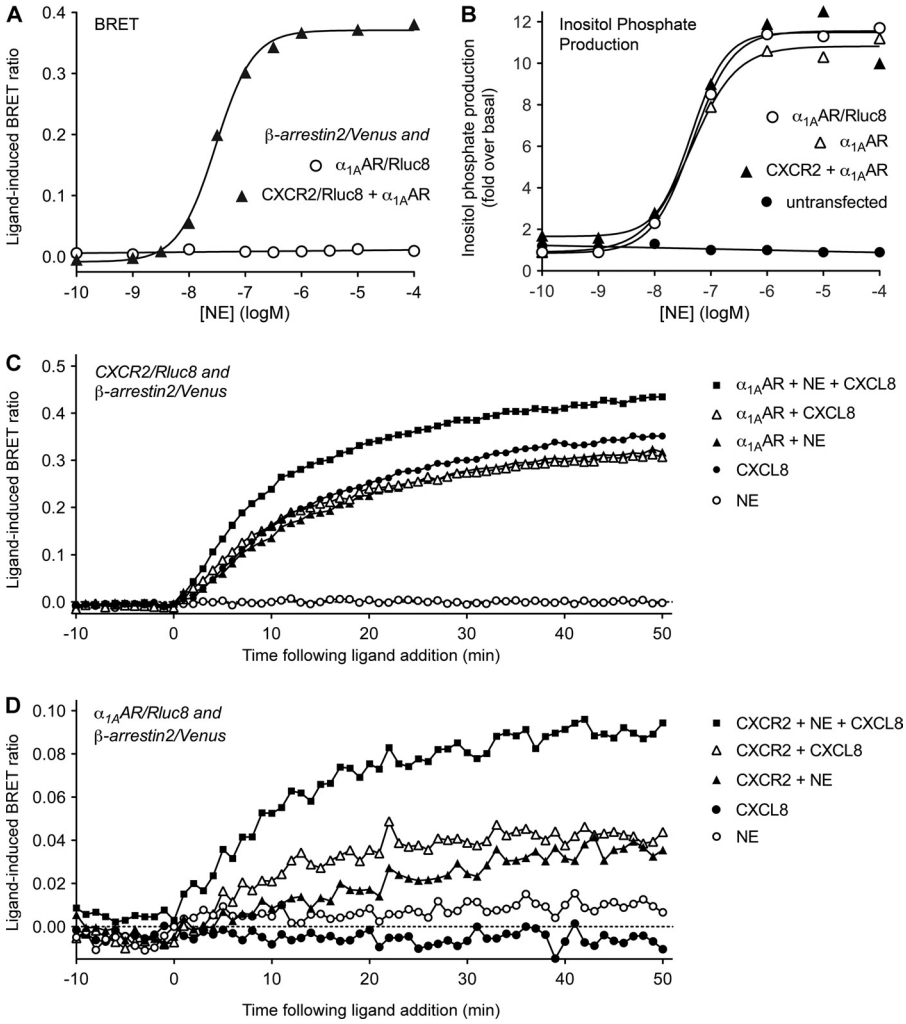

FIGURE 2. **Profiling of the novel α_{1A}AR-CXCR2 heteromer.** HEK293FT cells co-expressing β-arrestin2/Venus with either α_{1A}AR/Rluc8 only or CXCR2/Rluc8 and α_{1A}AR were monitored at 37 °C using BRET to generate dose-response curves (*A*). The mean BRET EC_{50} value ± S.E. for the CXCR2/Rluc8 and α_{1A}AR combination was 29.7 ± 2.1 nM, and the mean Hill slope ± S.E. was 1.4 ± 0.1. Total inositol phosphate signaling dose-response curves were also generated to demonstrate the functionality of α_{1A}AR/Rluc8 compared with untagged α_{1A}AR and to compare the signaling of α_{1A}AR in the presence and absence of CXCR2 (*B*). The mean EC_{50} values ± S.E. were not significantly different for α_{1A}AR/Rluc8 and α_{1A}AR co-expressed with CXCR2 compared with α_{1A}AR ($p > 0.05$) and were 30.1 ± 11.6, 86.3 ± 45.6, and 52.2 ± 14.9 nM, respectively (statistics carried out using logEC_{50} values). Extended BRET (eBRET) kinetic profiles (35, 67) were generated with cells co-expressing CXCR2/Rluc8 and β-arrestin2/Venus with or without α_{1A}AR and activated with 100 nM CXCL8 and/or 100 μM NE (*C*). Profiles were also generated with cells co-expressing α_{1A}AR/Rluc8 and β-arrestin2/Venus with or without CXCR2 (*D*). Data are representative of at least three independent experiments.

with either Terazosin or SB265610 alone (Fig. 4*B*). The categorization of SB265610 as an inverse agonist (44) is supported by the reduction in basal ligand-induced BRET ratio over time (Fig. 4, *A* and *B*).

The inhibition of both CXCL8- and NE-induced BRET signals by SB265610 indicates a critical role for CXCR2 in β-arrestin2 recruitment to the α_{1A}AR-CXCR2 heteromer regardless of which receptor is initially activated by agonist.

Specificity of β-Arrestin Recruitment to α_{1A}AR-CXCR2 Heteromer—NE-induced β-arrestin recruitment shows specificity for the α_{1A}AR-CXCR2 heteromer (Fig. 5*A*), as it is not observed when untagged α_{1A}AR is co-expressed with various other Rluc8-tagged GPCRs, including chemokine receptor CCR2 (Fig. 5*B*), vasopressin receptor 2 (*V2R*, Fig. 5*C*) and orexin receptor 1 (*OxR1*, Fig. 5*D*). Luminescence and fluorescence values were similar for the different combinations, indicating similar expression of Rluc8 and Venus-tagged proteins (Fig. 5*E*). NE-induced inositol phosphate production was also similar for each combination, indicating similar expression of α_{1A}AR (Fig. 5*F*). The proximity/orientation dependence of BRET is such that a lack of BRET signal does not necessarily mean a lack of proximity between proteins of interest (46), but it is at least consistent with this situation. It is also important to note that a receptor could be in close proximity to α_{1A}AR without altering its pharmacology (in this case without enabling NE-induced β-arrestin recruitment).

Assessment of BRET between Receptors—BRET saturation assays were carried out to compare with the findings from the GPCR-HIT assay, assessing the α_{1A}AR and CXCR2 combination as well as the α_{1A}AR and V2R combination as a control. A saturation curve with a $BRET_{max}$ of 0.96 was fitted to the data with α_{1A}AR/Rluc8 and CXCR2/Venus, consistent with these receptors being in close proximity in a constitutive heteromer (Fig. 6*A*). Surprisingly, despite no NE-induced β-arrestin

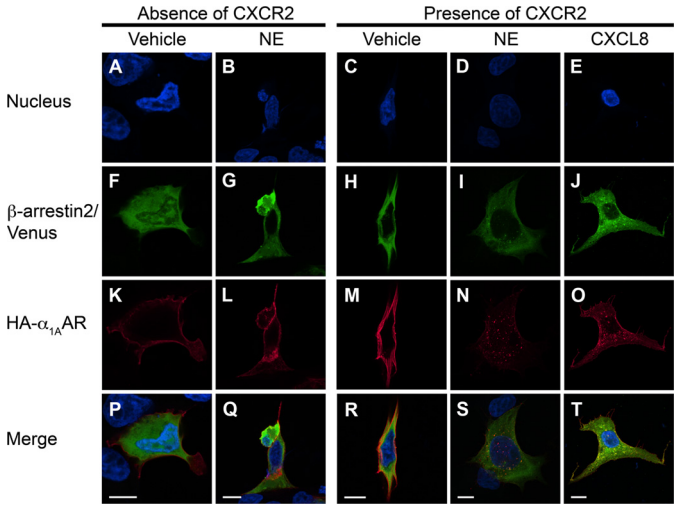

FIGURE 3. **β-Arrestin2/Venus translocation and HA-α_{1A}AR internalization studies on cells with or without untagged CXCR2.** HEK293FT cells were visualized using confocal microscopy to observe the nuclei with Hoechst staining (*blue*, *A–E*), β-arrestin2/Venus localization (*green*, *F–J*), HA-α_{1A}AR localization (*red*, *K–O*), and merged images of all three (*P–T*). Cells expressing β-arrestin2/Venus and HA-α_{1A}AR were treated with vehicle (*A*, *F*, *K*, and *P*) or 100 nM NE (*B*, *G*, *L*, and *Q*) for 30 min. Similarly, cells expressing β-arrestin2/Venus, HA-α_{1A}AR, and untagged CXCR2 were treated with vehicle (*C*, *H*, *M*, and *R*) or 100 nM NE (*D*, *I*, *N*, and *S*) or 100 nM CXCL8 (*E*, *J*, *O*, and *T*) for 30 min. Scale bars, 10 μm.

recruitment being observed with GPCR-HIT with V2R/Rluc8, β-arrestin2/Venus, and α_{1A}AR (Fig. 5*C*), the α_{1A}AR/Rluc8 and V2R/Venus combination resulted in a saturation curve with a $BRET_{max}$ of 1.22 (Fig. 6*A*). This is consistent with V2R being in close proximity to α_{1A}AR in these cells yet not modulating α_{1A}AR pharmacology to enable NE to induce β-arrestin recruitment. This further illustrates the specificity of the GPCR-HIT assay due to its dependence upon a ligand-induced functional effect.

One possible explanation for the inhibition of the ligand-induced BRET signals observed in Fig. 4 by Terazosin and/or SB265610 is that the heteromer is disrupted by treatment with these ligands. However, the constitutive BRET signal between α_{1A}AR/Rluc8 and CXCR2/Venus was not altered by treatment with Terazosin, SB265610, or a combination of both (Fig. 6*B*). The effect of CXCL8 and NE was also assessed, and again no change in BRET signal was observed (Fig. 6*C*).

Effect of Inhibitors on NE-induced Inositol Phosphate Production—In contrast to BRET investigating β-arrestin recruitment, NE-induced inositol phosphate production was completely inhibited by Terazosin but was unaffected by SB265610 (Fig. 7). Note that, crucially, the NE-induced BRET signal observed is specific for the heteromer, whereas the NE-induced inositol phosphate signal could result from activation of either α_{1A}AR-CXCR2 heteromers or α_{1A}AR monomers/homomers. Therefore, the lack of inhibition by SB265610 could be explained by the ability of α_{1A}AR to recruit G protein to the heteromer even when CXCR2 is in an inactive conformation, implying recruitment of the G protein directly to the activated α_{1A}AR protomer. Alternatively or additionally, the inositol phosphate production observed may result from activation of α_{1A}AR monomers/homomers, as the inositol phosphate assay cannot distinguish between these receptor populations.

Evidence for Labetalol Exhibiting Heteromer-specific Biased Agonism—Upon preliminary testing of a selection of adrenoceptor-selective compounds, agonist activity was observed with Labetalol, which is marketed as a nonselective β-AR antagonist with α_1AR antagonist properties. As partial agonist activity at β-ARs had been observed previously with this compound (47, 48) but to our knowledge not at α-ARs, we profiled this particular compound further. Similarly to NE, a very strong dose-dependent BRET signal was observed after Labetalol treatment of cells expressing β-arrestin2/Venus, CXCR2/Rluc8, and untagged α_{1A}AR, in contrast to the distinct lack of BRET signal with cells expressing β-arrestin2/Venus and α_{1A}AR/Rluc8 (Fig. 8*A*). From the same transfections, Labetalol-induced dose-dependent inositol phosphate production was observed with both combinations (Fig. 8*B*), indicating that like NE, Labetalol acting on the α_{1A}AR monomer/homomer is able to induce G protein-coupling but little or no β-arrestin recruitment. We then investigated the relative levels of agonism of Labetalol for β-arrestin recruitment and inositol phosphate production compared with NE. For β-arrestin, Labetalol was almost a full agonist compared with NE, with 10 μM Labetalol preincubation resulting in only a marginal reduction in NE response (Fig. 8*C*). In contrast, Labetalol was only a partial agonist for inositol phosphate signaling, a 10 μM dose substantially reducing the response to doses of NE ≤ 1 μM and shifting the NE EC_{50} >1300-fold to the right (Fig. 8*D*). Furthermore, as inositol phosphate assays cannot distinguish between coupling to the receptor heteromer complex *versus* the α_{1A}AR monomer/homomer, it is unclear what proportions of these signals if any are due to the α_{1A}AR-CXCR2 complex rather than the α_{1A}AR monomer/homomer (Fig. 8*B*). Therefore, if anything, these data overestimate the amount of Labetalol agonism at the receptor complex for the $G_{q/11}$ signaling pathway.

Extended BRET (eBRET) kinetic profiles were generated using submaximal concentrations of NE and Labetalol (Fig. 8*E*). The addition of 10 μM Labetalol had little effect on the BRET signal resulting from 100 nM NE, in contrast to the effect of 10 μM Terazosin on the NE-induced BRET (Fig. 8*E*). The agonism of 300 nM Labetalol with respect to β-arrestin recruitment to the receptor complex was clearly observed and was inhibited by 10 μM Terazosin, which exhibited no agonism on its own. Together, these data indicate that although Labetalol is a partial agonist for inositol phosphate signaling from α_{1A}AR, it is effectively a full agonist for β-arrestin recruitment to the α_{1A}AR-CXCR2 complex, thereby defining it as a β-arrestin-biased ligand (49).

DISCUSSION

We have provided evidence for CXCR2 expression in the prostate stroma, a region specifically associated with α_{1A}AR expression *in vivo* (25). Visualization of the α_{1A}AR was not carried out due to the lack of reliable α_{1A}AR antibodies (50). We then proceeded to demonstrate a "biochemical fingerprint" of the α_{1A}AR-CXCR2 heteromer by uncovering novel and specific pharmacology attributable to the heteromer complex in HEK293 cells. This has been done primarily using a BRET-based approach, which although not giving absolute proof of direct physical association between the receptors, does provide

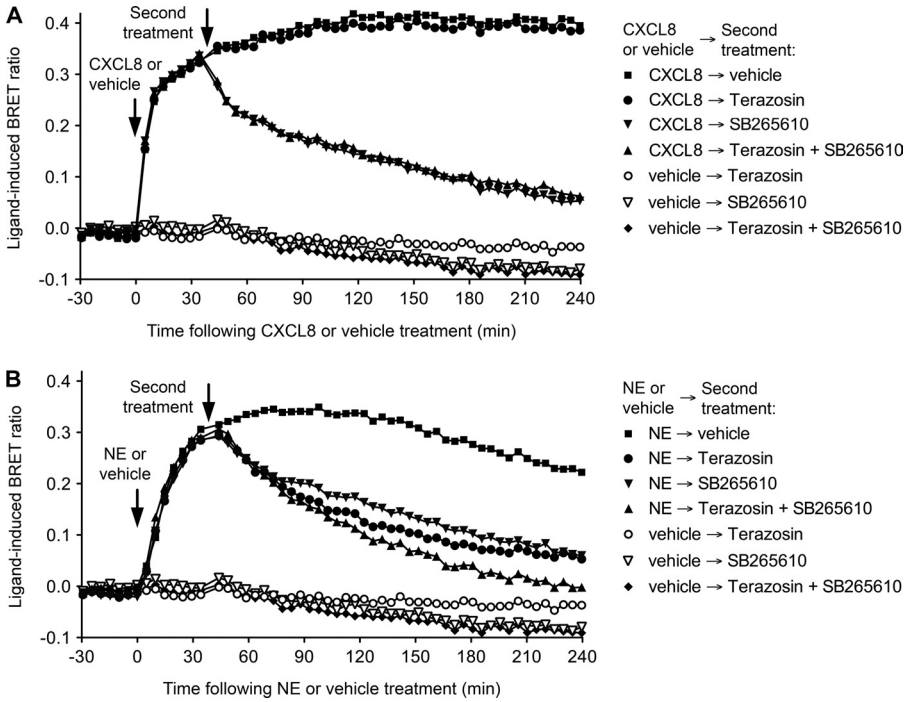

FIGURE 4. **Use of Terazosin (α_1AR antagonist) and SB265610 (CXCR2 inverse agonist) to interrogate β-arrestin2/Venus recruitment.** eBRET kinetic profiles were generated for the CXCR2/Rluc8, β-arrestin2/Venus and α_{1A}AR combination in HEK293FT cells by treating with CXCL8 or vehicle (*A*) or NE or vehicle (*B*) ~30 min before a second treatment with vehicle, 10 μM Terazosin, and/or 10 μM SB265610. Data are representative of three independent experiments.

strong evidence of both functional interaction and close proximity in a "macromolecular complex."

Using GPCR-HIT, we have shown that α_{1A}AR, which has been published to interact with β-arrestin very weakly if at all in transfected HEK293 cells (30), can recruit and form a stable complex with β-arrestin when it is co-expressed with CXCR2, but not CCR2, V2R, or OxR1. Indeed, it even appears that co-expression of V2R does not have this effect despite specific close proximity with α_{1A}AR in these cells as suggested by BRET saturation assays. Our evidence for α_{1A}AR-CXCR2 complex formation with β-arrestin provided from BRET-based assays has been supported by visualization of co-localization using confocal microscopy. Indeed, the observation of CXCL8 causing α_{1A}AR internalization is particularly compelling, especially as NE was not seen to induce internalization of α_{1A}AR in the absence of CXCR2. Indeed, this nicely illustrates a role CXCR2 may play in regulating α_{1A}AR.

Intriguingly, not only the α_1AR antagonist Terazosin but also the CXCR2-specific inverse agonist SB265610 was observed to inhibit NE-induced β-arrestin recruitment to the receptor complex. This inhibition does not appear to be due to disruption of the heteromer as such, as treatment with Terazosin, SB265610, or both did not inhibit the BRET signal between α_{1A}AR/Rluc8 and CXCR2/Venus. Indeed, agonist treatment also did not affect the BRET between receptors, implying that heteromerization in this particular case occurs constitutively. Therefore, the observed inhibition of the GPCR-HIT BRET signals is likely to be due to blockade of receptor activation, blockade of actual β-arrestin2/Venus binding to the complex, and/or blockade of an allosteric effect across the complex that facilitates β-arrestin recruitment to the heteromer.

There has been debate in the literature for several years regarding whether or not GPCR heteromerization, and indeed homomerization, is constitutive or ligand-modulated. Not that long ago most homo- and heteromerization was believed to occur constitutively, with receptors forming complexes in the endoplasmic reticulum and trafficking to the plasma membrane together (51) as well as internalizing together (52). More recently, evidence has been presented of examples where homo- and heteromerization appears to be more dynamic (53, 54). Indeed BRET, including in the GPCR-HIT configuration, has recently been used to investigate the heteromer between the gastric inhibitory polypeptide (GIP) receptor and glucagon-like peptide-1 (GLP-1) receptor, with the authors proposing a model of dynamic heteromer formation induced by GLP-1 and dissolved by GIP (55). Furthermore GPCR-HIT in this case, as it has in our current study, enabled conclusions to be drawn regarding functional implications of heteromerization with respect to β-arrestin recruitment. Interestingly, the difference is that α_{1A}AR-CXCR2 appears to be a constitutively formed heteromer that recruits β-arrestin in contrast to the α_{1A}AR monomer/homomer, whereas the GIP receptor-GLP-1 receptor heteromer appears to form dynamically, with the heteromer recruiting β-arrestin less well than the GLP-1 receptor monomer/homomer (55). These differences illustrate that the novel pharmacology resulting from GPCR heteromerization can take various forms even just in terms of β-arrestin recruitment and can differ for each individual combination of receptors.

Our findings suggest that an allosteric effect occurs between α_{1A}AR and CXCR2 that modulates the functioning of the constitutively formed heteromer complex with regard to β-arrestin recruitment. There are essentially three potential scenarios for

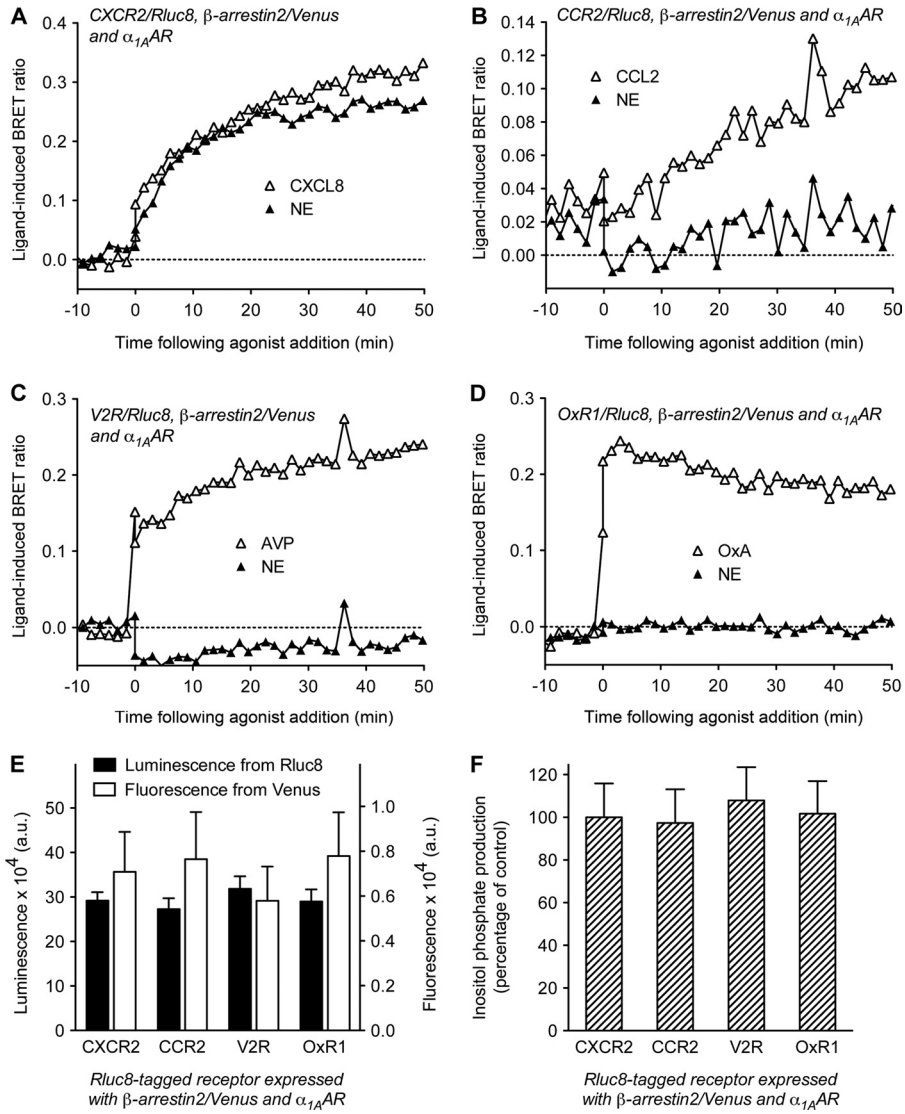

FIGURE 5. **Specificity of β-arrestin recruitment to the α_{1A}AR-CXCR2 heteromer.** eBRET kinetic profiles were generated with HEK293FT cells expressing β-arrestin2/Venus and α_{1A}AR with CXCR2/Rluc8 (*A*), CCR2/Rluc8 (*B*), V2R/Rluc8 (*C*), or OxR1/Rluc8 (*D*). Cells were treated with the agonist for the Rluc8-tagged GPCR (100 nM) or NE (100 nM). Data are representative of at least three independent experiments. *AVP*, arginine vasopressin. *OxA*, Orexin A. Luminescence and fluorescence values were recorded for the different combinations (*E*) as well as NE-induced inositol phosphate production (*F*). Data in *F* are shown as a percentage of the signal generated by NE-treated CXCR2/Rluc8, β-arrestin2/Venus, and α_{1A}AR-expressing cells (control, *first column*). For *E* and *F*, data are shown as the mean ± S.E. of at least three independent experiments carried out with the same transfections as used to generate the data for *A*–*D*.

explaining our observations upon stimulation with NE, depending upon whether the β-arrestin2 associates with the α_{1A}AR-CXCR2 heteromer via interaction with CXCR2, α_{1A}AR, or both. The concept of asymmetric activation of GPCR heteromers is being increasingly recognized and has been discussed recently (56, 57), so multiple scenarios are plausible.

The first scenario, which we will term the "trans hypothesis," involves NE-bound α_{1A}AR allosterically activating (or transactivating) CXCR2 that in turn binds β-arrestin2 (Fig. 9*B*). In this case, agonist binding to one of the protomers results in the activation of both protomers in the heteromer. This would account for the substantially weaker BRET signals obtained when the α_{1A}AR is labeled rather than CXCR2 (Fig. 2). As the BRET signal is inversely proportional to distance to the sixth power (58), NE-induced recruitment of β-arrestin2/Venus to interact with CXCR2/Rluc8 (Fig. 9*C*) would be expected to result in a much larger signal than recruiting β-arrestin2/Venus to interact with untagged CXCR2 (Fig. 9*D*), with the energy transfer then occurring across the complex from α_{1A}AR/Rluc8. Arguably "trans" β-arrestin recruitment to CXCR2 in the α_{1A}AR-CXCR2 heteromer is also consistent with the ability of not only the α_1AR antagonist Terazosin (Fig. 9*F*) but also the CXCR2-specific inverse agonist SB265610 (Fig. 9*H*) to block NE-induced β-arrestin recruitment to the receptor complex.

The second scenario, which we will term the "cis hypothesis," involves CXCR2 allosterically modulating the α_{1A}AR as a consequence of heteromerization, with the result that NE-activated α_{1A}AR is able to bind β-arrestin2 with high affinity when it could not as a monomer/homomer. Despite α_{1A}AR containing two putative high affinity GPCR kinase (GRK) phosphorylation sites as defined by Oakley *et al.* (59, 60), it is phosphorylated much more weakly than α_{1B}AR, which contains none of

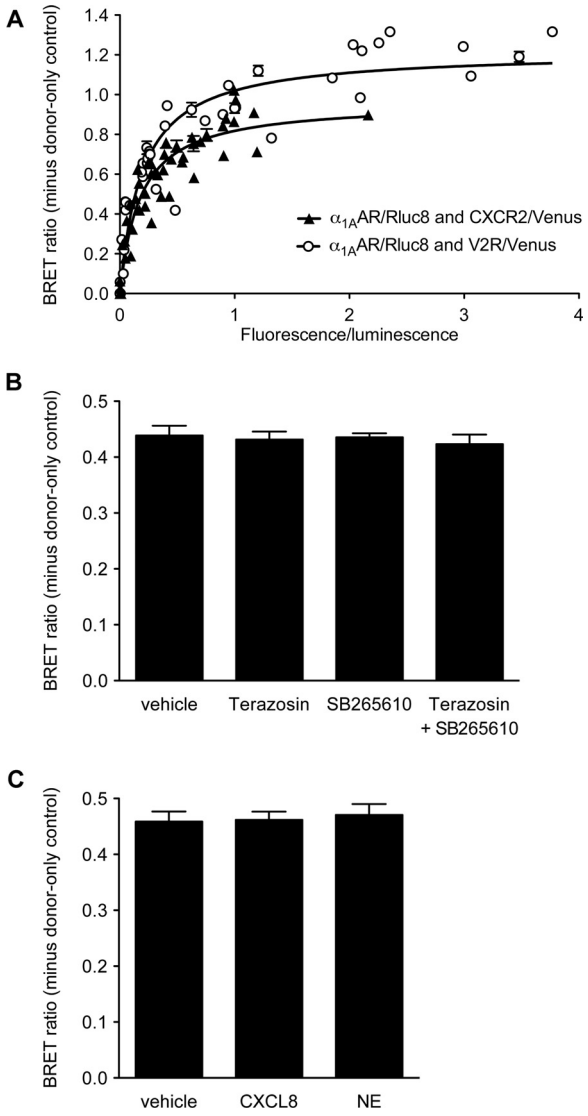

FIGURE 6. **Assessment of BRET between receptors.** Saturation BRET data were generated with HEK293FT cells co-expressing α_{1A}AR/Rluc8 with either CXCR2/Venus or V2R/Venus (*A*). The graph was generated by combining data from four independent experiments carried out in triplicate (*error bars* represent mean ± S.E. of triplicate data). Cells transfected with equal amounts of α_{1A}AR/Rluc8 and CXCR2/Venus cDNA were treated for 20 min with vehicle, 10 μM Terazosin, 10 μM SB265610, or both (*B*). Similarly, cells were treated for 20 min with vehicle, 100 nM CXCL8, or 100 nM NE (*C*). Data for *B* and *C* shown as the mean ± S.E. of three independent experiments. Data are presented as *BRET ratio (minus donor-only control)* to assess the constitutive BRET signal between the receptors.

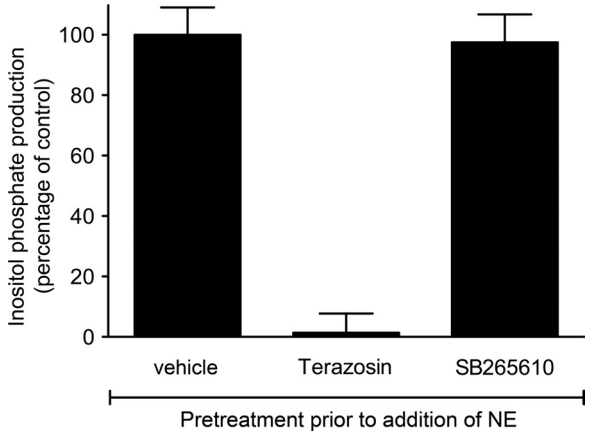

FIGURE 7. **Effect of Terazosin and SB265610 on NE-induced inositol phosphate production from cells expressing α_{1A}AR and CXCR2.** Data are shown as the mean ± S.E. of three independent experiments generated from the same transfections of HEK293FT cells co-expressing CXCR2/Rluc8, β-arrestin2/Venus, and α_{1A}AR used to generate data shown in Fig. 4. Data are shown as a percentage of the signal generated by NE-treated cells pretreated with vehicle (control, *first column*).

these serine/threonine clusters in the C-terminal tail (61). This difference in phosphorylation is consistent with the difference in β-arrestin recruitment observed between the two receptor subtypes (30). Both of these observations are, therefore, counterintuitive but can be explained by recent studies that have provided evidence for differential GPCR phosphorylation resulting in a signaling "bar code" (62–65). This is the concept that, depending on the cellular context or even the ligand used to activate the receptor, distinct subsets of potential sites are phosphorylated, thereby enabling an additional layer of signaling diversity to be achieved depending on the particular receptor conformation and set of conditions (62–65). Therefore, an allosteric effect of CXCR2 that changes the α_{1A}AR conformation could conceivably alter the phosphorylation bar code, enabling the α_{1A}AR to be differentially phosphorylated and thereby changing its affinity for β-arrestin2. If this is the reality, the explanation for the different strength of BRET signals in the two tag orientations (Fig. 9, *C* and *D*) would presumably be attributed to the orientation involving α_{1A}AR/Rluc8 (Fig. 9*D*) simply being much less favorable for energy transfer. Furthermore, as a consequence of its binding to the C-terminal tail of CXCR2, SB265610 may be able to influence a putative allosteric effect of CXCR2 on α_{1A}AR that alters the phosphorylation bar code on the α_{1A}AR C-terminal tail, thereby indirectly inhibiting β-arrestin2 binding to α_{1A}AR. The third possibility is that β-arrestin2 interacts with binding sites on both protomers in the heteromer, which would again imply an alteration of the phosphorylation bar code on α_{1A}AR to enable this to occur.

Our findings can also be considered in terms of biased signaling. Indeed, the observed heteromer-biased β-arrestin recruitment reflects the difference between α_{1A}AR being a G protein-biased receptor and the α_{1A}AR-CXCR2 heteromer being unbiased (24). In terms of ligand-bias in the heteromer context, we have identified Labetalol as exhibiting such properties.

In a clinical setting, Labetalol is utilized for its antagonism of adrenoceptors, and in terms of inositol phosphate production, this *in vivo* effect is supported by the relatively weak partial agonism observed. However, although studies have indicated a lack of Labetalol-induced β-arrestin recruitment to the β_2AR (48), our findings indicate strong Labetalol-induced β-arrestin recruitment to the α_{1A}AR-CXCR2 heteromer, highlighting that the concept of heteromerization needs to be taken into account when investigating ligand-biased signaling. Indeed, the allosterism between the receptors that is proposed to enable β-arrestin recruitment to the heteromer after α_{1A}AR activation is likely to facilitate the ability of Labetalol to act as a biased full agonist for β-arrestin recruitment, thereby potentially explaining why biased agonism was not observed with the β_2AR monomer/homomer.

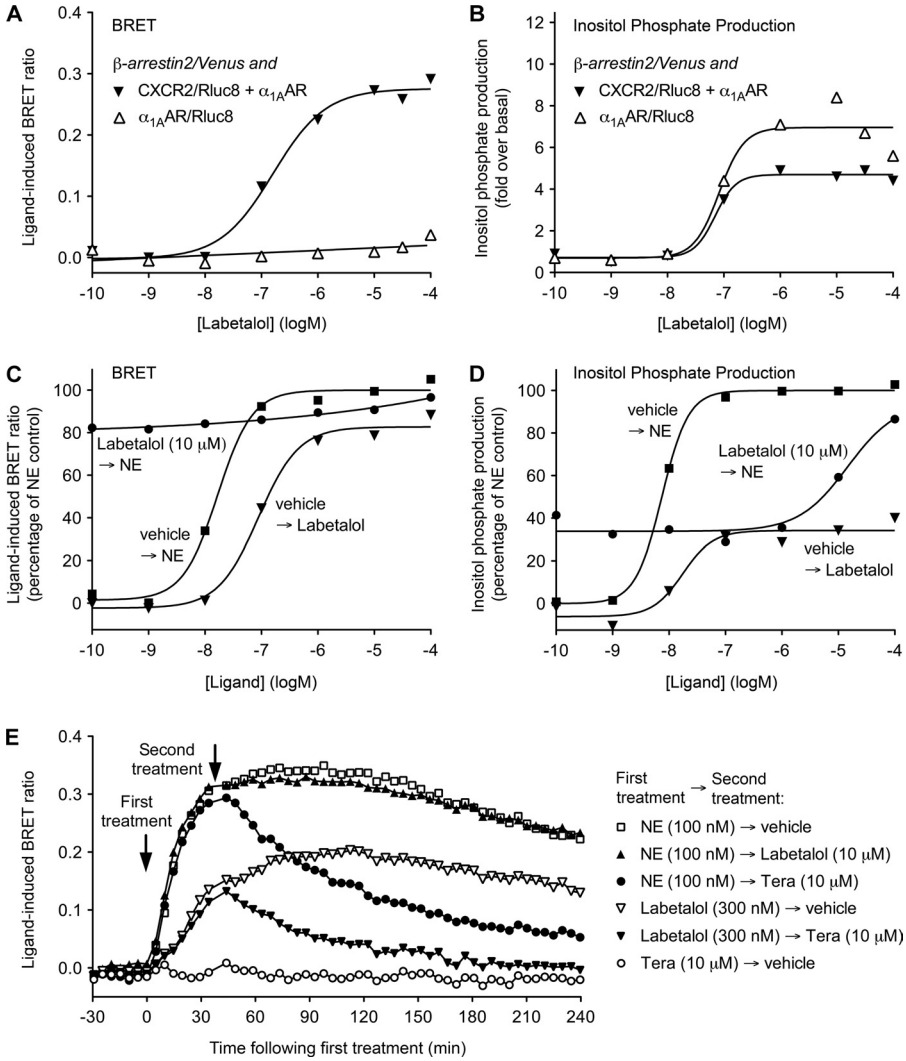

FIGURE 8. **Comparison of Labetalol and NE treatment on β-arrestin2/Venus recruitment and inositol phosphate production.** HEK293FT cells co-expressing β-arrestin2/Venus with either α_{1A}AR/Rluc8 or CXCR2/Rluc8 and α_{1A}AR were monitored at 37 °C for BRET (*A*) and inositol phosphate production (*B*) to generate dose-response curves. In a separate set of experiments, dose-response curves for BRET (*C*) and inositol phosphate production (*D*) were generated with the same transfection of HEK293FT cells transiently co-expressing CXCR2/Rluc8, β-arrestin2/Venus, and α_{1A}AR. For both, preincubation with 10 μM Labetalol or vehicle for 20 min was followed by activation with increasing doses of NE or Labetalol as indicated for 40 min. For comparison, both *C* and *D* have been presented as percentage of response to NE in the absence of Labetalol treatment (NE control). The mean BRET EC_{50} values ± S.E. for NE and Labetalol (with vehicle preincubation) were 16.2 ± 1.6 and 96.2 ± 10.1 nM, respectively. The mean inositol phosphate production EC_{50} values ± S.E. for NE with vehicle preincubation, Labetalol with vehicle preincubation, and NE with Labetalol preincubation were 7.1 ± 1.6, 19.9 ± 6.6, and 9634 ± 2495 nM, respectively. eBRET kinetic profiles were generated for the CXCR2/Rluc8, β-arrestin2/Venus, and α_{1A}AR combination (*E*), showing the effect of 10 μM Labetalol compared with 10 μM Terazosin (*Tera*) when added ~30 min after activation by a submaximal dose of NE (100 nM). The effect of a submaximal dose of Labetalol (300 nM) with or without subsequent 10 μM Terazosin treatment is also shown along with the effect of 10 μM Terazosin alone. Data are representative of three independent experiments.

Whether the biased agonism of Labetalol is clinically relevant (unwanted or fortuitous) is far from clear and requires extensive investigation, as the precise mechanism of action of Labetalol is itself not fully elucidated. This was illustrated when an infant was accidentally given a massive overdose with amazingly limited clinical effect (66). The explanation was unclear, although altered distribution or structure of α-ARs was suggested as possibly playing a role. More generally, the potential clinical relevance of biased agonism is becoming increasingly apparent, with recent work from Lefkowitz and co-workers (48) implicating a role for β-arrestin signaling via adrenoceptors in the regulation of apoptosis. Our demonstration of heteromer-biased β-arrestin recruitment takes these important concepts one step further.

We postulate that heteromerization provides another mechanism by which α_{1A}AR can exhibit distinct pharmacological profiles and consequently exert its diverse biological effects. Indeed, such heteromerization may account for the recent evidence of α_{1A}AR-β-arrestin2 complex formation specifically in the prostate stroma (31) despite the poor interaction observed in transfected HEK293 cells (30). More broadly, we suggest that heteromerization provides a mechanism by which certain GPCRs can either form a functional complex with β-arrestin without necessarily physically interacting with the protein themselves or alter their own ability to interact with β-arrestin. Therefore, these concepts and the approaches used to investigate them have substantial implications for the wider GPCR field and for drug discovery at these important pharmaceutical targets.

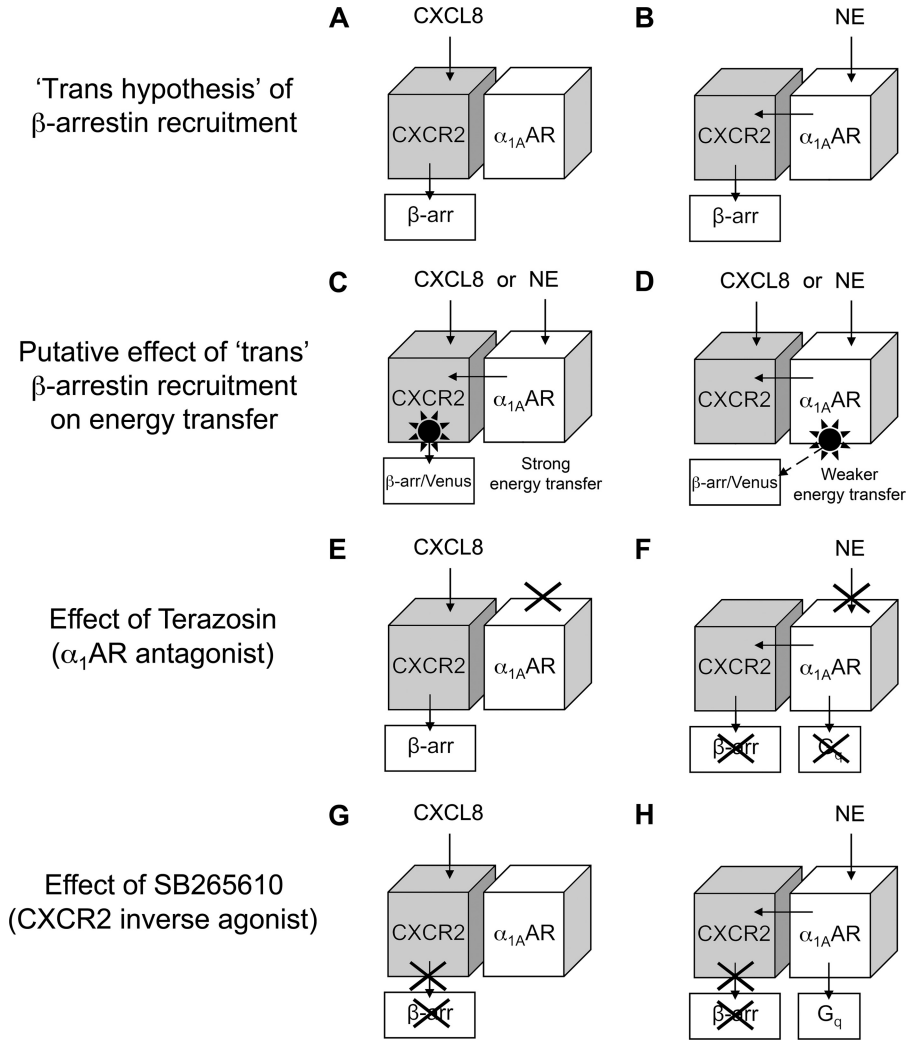

FIGURE 9. **Model of trans hypothesis of β-arrestin recruitment to the α_{1A}AR-CXCR2 heteromer.** CXCL8 activation of CXCR2 results in recruitment of β-arrestin2 (*β-arr*) to CXCR2, which may or may not heteromerize with α_{1A}AR (*A*). One hypothesis to explain our observations after NE treatment is that NE activation of α_{1A}AR results in β-arrestin2 recruitment to the α_{1A}AR-CXCR2 heteromer via interaction with CXCR2 (*B*). Consistent with this hypothesis are the different strengths of energy transfer shown in Fig. 2 depending upon whether the Rluc8 fusion (*black star*) is with CXCR2 (*C*) or α_{1A}AR (*D*). In terms of inhibitor treatments, Terazosin did not affect CXCL8-induced recruitment of β-arrestin2 to CXCR2 (*E*); however, it did inhibit both NE-induced $G_{q/11}$ coupling and β-arrestin2 recruitment (*F*). In contrast, SB265610 inhibited both CXCL8-induced (*G*) and NE-induced (*H*) β-arrestin2 recruitment without apparently affecting $G_{q/11}$ coupling, although unlike GPCR-HIT, the measurement of inositol phosphate production does not discriminate between α_{1A}AR monomers/homomers and α_{1A}AR-CXCR2 heteromers.

Acknowledgments—We acknowledge the facilities and scientific and technical assistance of the Australian Microscopy and Microanalysis Research Facility at the Centre for Microscopy, Characterization, and Analysis, The University of Western Australia, a facility funded by the University, State, and Commonwealth Governments.

REFERENCES

1. Kenakin, T. P. (2009) Cellular assays as portals to seven-transmembrane receptor-based drug discovery. *Nat. Rev. Drug Discov.* **8,** 617–626
2. Ferré, S., Baler, R., Bouvier, M., Caron, M. G., Devi, L. A., Durroux, T., Fuxe, K., George, S. R., Javitch, J. A., Lohse, M. J., Mackie, K., Milligan, G., Pfleger, K. D., Pin, J. P., Volkow, N. D., Waldhoer, M., Woods, A. S., and Franco, R. (2009) Building a new conceptual framework for receptor heteromers. *Nat. Chem. Biol.* **5,** 131–134
3. Whorton, M. R., Bokoch, M. P., Rasmussen, S. G., Huang, B., Zare, R. N., Kobilka, B., and Sunahara, R. K. (2007) A monomeric G protein-coupled receptor isolated in a high density lipoprotein particle efficiently activates its G protein. *Proc. Natl. Acad. Sci. U.S.A.* **104,** 7682–7687
4. Ernst, O. P., Gramse, V., Kolbe, M., Hofmann, K. P., and Heck, M. (2007) Monomeric G protein-coupled receptor rhodopsin in solution activates its G protein transducin at the diffusion limit. *Proc. Natl. Acad. Sci. U.S.A.* **104,** 10859–10864
5. Whorton, M. R., Jastrzebska, B., Park, P. S., Fotiadis, D., Engel, A., Palczewski, K., and Sunahara, R. K. (2008) Efficient coupling of transducin to monomeric rhodopsin in a phospholipid bilayer. *J. Biol. Chem.* **283,** 4387–4394
6. Kuszak, A. J., Pitchiaya, S., Anand, J. P., Mosberg, H. I., Walter, N. G., and Sunahara, R. K. (2009) Purification and functional reconstitution of monomeric μ-opioid receptors. Allosteric modulation of agonist binding by G_{i2}. *J. Biol. Chem.* **284,** 26732–26741
7. Eckert, R. E., Schreier, U., Drescher, P., Madsen, P. O., Derouet, H., Becht, E., Steffens, J., and Ziegler, M. (1995) Regulation of prostatic smooth muscle contractility by intracellular second messengers. Implications for the conservative treatment of benign prostatic hyperplasia. *Urol. Int.* **54,** 6–21
8. Muramatsu, I., Oshita, M., Ohmura, T., Kigoshi, S., Akino, H., Gobara, M., and Okada, K. (1994) Pharmacological characterization of α1-adrenoceptor subtypes in the human prostate. Functional and binding studies. *Br. J. Urol.* **74,** 572–578

9. Ford, A. P., Arredondo, N. F., Blue, D. R., Jr., Bonhaus, D. W., Jasper, J., Kava, M. S., Lesnick, J., Pfister, J. R., Shieh, I. A., Vimont, R. L., Williams, T. J., McNeal, J. E., Stamey, T. A., and Clarke, D. E. (1996) RS-17053 (*N*-[2-(2-cyclopropylmethoxyphenoxy)ethyl]-5-chloro-α,α-dimethyl-1H-indole-3-ethanamine hydrochloride), a selective α 1A-adrenoceptor antagonist, displays low affinity for functional α 1-adrenoceptors in human prostate. implications for adrenoceptor classification. *Mol. Pharmacol.* **49,** 209–215
10. Gray, K., Short, J., and Ventura, S. (2008) The α1A-adrenoceptor gene is required for the α1L-adrenoceptor-mediated response in isolated preparations of the mouse prostate. *Br. J. Pharmacol.* **155,** 103–109
11. Shibata, K., Hirasawa, A., Moriyama, N., Kawabe, K., Ogawa, S., and Tsujimoto, G. (1996) α1a-adrenoceptor polymorphism. Pharmacological characterization and association with benign prostatic hypertrophy. *Br. J. Pharmacol.* **118,** 1403–1408
12. Suzuki, F., Taniguchi, T., Takauji, R., Murata, S., and Muramatsu, I. (2000) Splice isoforms of α(1a)-adrenoceptor in rabbit. *Br. J. Pharmacol.* **129,** 1569–1576
13. Ramsay, D., Carr, I. C., Pediani, J., Lopez-Gimenez, J. F., Thurlow, R., Fidock, M., and Milligan, G. (2004) High affinity interactions between human α1A-adrenoceptor C-terminal splice variants produce homo- and heterodimers but do not generate the α1L-adrenoceptor. *Mol. Pharmacol.* **66,** 228–239
14. Muramatsu, I., Tanaka, T., Suzuki, F., Li, Z., Hiraizumi-Hiraoka, Y., Anisuzzaman, A. S., Yamamoto, H., Horinouchi, T., and Morishima, S. (2005) Quantifying receptor properties. The tissue segment binding method; a powerful tool for the pharmacome analysis of native receptors. *J. Pharmacol. Sci.* **98,** 331–339
15. Nishimune, A., Suzuki, F., Yoshiki, H., Morishima, S., and Muramatsu, I. (2010) α1-Adrenoceptor pharmacome. α1L-adrenoceptor and α1A-adrenoceptor in the lower urinary tract. *Int. J. Urol.* **17,** 31–37
16. Nishimune, A., Suzuki, F., Yoshiki, H., Morishima, S., and Muramatsu, I. (2010) Identification of cysteine-rich epidermal growth factor-like domain 1α (CRELD1α) as a novel α1A-adrenoceptor-down-regulating protein and establishment of an α1L-adrenoceptor-expressing cell line. *J. Pharmacol. Sci.* **113,** 169–181
17. Uberti, M. A., Hall, R. A., and Minneman, K. P. (2003) Subtype-specific dimerization of α 1-adrenoceptors. Effects on receptor expression and pharmacological properties. *Mol. Pharmacol.* **64,** 1379–1390
18. LaRocca, T. J., Schwarzkopf, M., Altman, P., Zhang, S., Gupta, A., Gomes, I., Alvin, Z., Champion, H. C., Haddad, G., Hajjar, R. J., Devi, L. A., Schecter, A. D., and Tarzami, S. T. (2010) β2-Adrenergic receptor signaling in the cardiac myocyte is modulated by interactions with CXCR4. *J. Cardiovasc. Pharmacol.* **56,** 548–559
19. Cotecchia, S. (2010) The α1-adrenergic receptors. Diversity of signaling networks and regulation. *J. Recept. Signal. Transduct. Res.* **30,** 410–419
20. Acosta, J. C., O'Loghlen, A., Banito, A., Guijarro, M. V., Augert, A., Raguz, S., Fumagalli, M., Da Costa, M., Brown, C., Popov, N., Takatsu, Y., Melamed, J., d'Adda di Fagagna, F., Bernard, D., Hernando, E., and Gil, J. (2008) Chemokine signaling via the CXCR2 receptor reinforces senescence. *Cell* **133,** 1006–1018
21. Trettel, F., Di Bartolomeo, S., Lauro, C., Catalano, M., Ciotti, M. T., and Limatola, C. (2003) Ligand-independent CXCR2 dimerization. *J. Biol. Chem.* **278,** 40980–40988
22. Wilson, S., Wilkinson, G., and Milligan, G. (2005) The CXCR1 and CXCR2 receptors form constitutive homo- and heterodimers selectively and with equal apparent affinities. *J. Biol. Chem.* **280,** 28663–28674
23. Parenty, G., Appelbe, S., and Milligan, G. (2008) CXCR2 chemokine receptor antagonism enhances DOP opioid receptor function via allosteric regulation of the CXCR2-DOP receptor heterodimer. *Biochem. J.* **412,** 245–256
24. Mustafa, S., Ayoub, M. A., and Pfleger, K. D. (2010) Uncovering GPCR heteromer-biased ligands. *Drug Discov. Today: Technol.* **7,** e77–e85
25. Morishima, S., Suzuki, F., Nishimune, A., Yoshiki, H., Akino, H., Yokoyama, O., and Muramatsu, I. (2010) Visualization and tissue distribution of α1L-adrenoceptor in human prostate by the fluorescently labeled ligand Alexa-488-silodosin. *J. Urol.* **183,** 812–819
26. Ayoub, M. A., and Pfleger, K. D. (2010) Recent advances in bioluminescence resonance energy transfer technologies to study GPCR heteromerization. *Curr. Opin. Pharmacol.* **10,** 44–52
27. See, H. B., Seeber, R. M., Kocan, M., Eidne, K. A., and Pfleger, K. D. (2011) Application of G protein-coupled receptor-heteromer identification technology to monitor β-arrestin recruitment to G protein-coupled receptor heteromers. *Assay Drug Dev. Technol.* **9,** 21–30
28. Mustafa, S., and Pfleger, K. D. (2011) G protein-coupled receptor heteromer identification technology. Identification and profiling of GPCR heteromers. *J. Lab. Autom.* **16,** 285–291
29. Porrello, E. R., Pfleger, K. D., Seeber, R. M., Qian, H., Oro, C., Abogadie, F., Delbridge, L. M., and Thomas, W. G. (2011) Heteromerization of angiotensin receptors changes trafficking and arrestin recruitment profiles. *Cell. Signal.* **23,** 1767–1776
30. Stanasila, L., Abuin, L., Dey, J., and Cotecchia, S. (2008) Different internalization properties of the α1a- and α1b-adrenergic receptor subtypes. The potential role of receptor interaction with β-arrestins and AP50. *Mol. Pharmacol.* **74,** 562–573
31. Hennenberg, M., Schlenker, B., Roosen, A., Strittmatter, F., Walther, S., Stief, C., and Gratzke, C. (2011) β-Arrestin-2 is expressed in human prostate smooth muscle and a binding partner of α1A-adrenoceptors. *World J. Urol.* **29,** 157–163
32. Loening, A. M., Fenn, T. D., Wu, A. M., and Gambhir, S. S. (2006) Consensus guided mutagenesis of Renilla luciferase yields enhanced stability and light output. *Protein Eng. Des. Sel.* **19,** 391–400
33. Kocan, M., See, H. B., Seeber, R. M., Eidne, K. A., and Pfleger, K. D. (2008) Demonstration of improvements to the bioluminescence resonance energy transfer (BRET) technology for the monitoring of G protein-coupled receptors in live cells. *J. Biomol. Screen.* **13,** 888–898
34. Kocan, M., See, H. B., Sampaio, N. G., Eidne, K. A., Feldman, B. J., and Pfleger, K. D. (2009) Agonist-independent interactions between β-arrestins and mutant vasopressin type II receptors associated with nephrogenic syndrome of inappropriate antidiuresis. *Mol. Endocrinol.* **23,** 559–571
35. Pfleger, K. D., Dromey, J. R., Dalrymple, M. B., Lim, E. M., Thomas, W. G., and Eidne, K. A. (2006) Extended bioluminescence resonance energy transfer (eBRET) for monitoring prolonged protein-protein interactions in live cells. *Cell. Signal.* **18,** 1664–1670
36. Pfleger, K. D., Seeber, R. M., and Eidne, K. A. (2006) Bioluminescence resonance energy transfer (BRET) for the real-time detection of protein-protein interactions. *Nat. Protoc.* **1,** 337–345
37. Trinquet, E., Fink, M., Bazin, H., Grillet, F., Maurin, F., Bourrier, E., Ansanay, H., Leroy, C., Michaud, A., Durroux, T., Maurel, D., Malhaire, F., Goudet, C., Pin, J. P., Naval, M., Hernout, O., Chrétien, F., Chapleur, Y., and Mathis, G. (2006) D-*myo*-Inositol 1-phosphate as a surrogate of D-*myo*-inositol 1,4,5-tris phosphate to monitor G protein-coupled receptor activation. *Anal. Biochem.* **358,** 126–135
38. Wang, Y., Luo, W., and Reiser, G. (2007) Activation of protease-activated receptors in astrocytes evokes a novel neuroprotective pathway through release of chemokines of the growth-regulated oncogene/cytokine-induced neutrophil chemoattractant family. *Eur. J. Neurosci.* **26,** 3159–3168
39. Sugimoto, N., Rui, T., Yang, M., Bharwani, S., Handa, O., Yoshida, N., Yoshikawa, T., and Kvietys, P. R. (2008) Points of control exerted along the macrophage-endothelial cell-polymorphonuclear neutrophil axis by PE-CAM-1 in the innate immune response of acute colonic inflammation. *J. Immunol.* **181,** 2145–2154
40. Martínez Muñoz, L., Lucas, P., Navarro, G., Checa, A. I., Franco, R., Martínez-A, C., Rodríguez-Frade, J. M., and Mellado, M. (2009) Dynamic regulation of CXCR1 and CXCR2 homo- and heterodimers. *J. Immunol.* **183,** 7337–7346
41. Moldobaeva, A., and Wagner, E. M. (2005) Difference in proangiogenic potential of systemic and pulmonary endothelium. role of CXCR2. *Am. J. Physiol. Lung Cell Mol. Physiol.* **288,** L1117–L1123
42. Kojima, Y., Sasaki, S., Hayashi, Y., Tsujimoto, G., and Kohri, K. (2009) Subtypes of α1-adrenoceptors in BPH. Future prospects for personalized medicine. *Nat. Clin. Pract. Urol.* **6,** 44–53
43. Hieble, J. P., and Ruffolo, R. R., Jr. (1996) The use of α-adrenoceptor antagonists in the pharmacological management of benign prostatic hypertrophy. An overview. *Pharmacol. Res.* **33,** 145–160
44. Bradley, M. E., Bond, M. E., Manini, J., Brown, Z., and Charlton, S. J. (2009)

SB265610 is an allosteric, inverse agonist at the human CXCR2 receptor. *Br. J. Pharmacol.* **158,** 328–338
45. Salchow, K., Bond, M. E., Evans, S. C., Press, N. J., Charlton, S. J., Hunt, P. A., and Bradley, M. E. (2010) A common intracellular allosteric binding site for antagonists of the CXCR2 receptor. *Br. J. Pharmacol.* **159,** 1429–1439
46. Levoye, A., Dam, J., Ayoub, M. A., Guillaume, J. L., Couturier, C., Delagrange, P., and Jockers, R. (2006) The orphan GPR50 receptor specifically inhibits MT1 melatonin receptor function through heterodimerization. *EMBO J.* **25,** 3012–3023
47. Galandrin, S., and Bouvier, M. (2006) Distinct signaling profiles of β1 and β2 adrenergic receptor ligands toward adenylyl cyclase and mitogen-activated protein kinase reveals the pluridimensionality of efficacy. *Mol. Pharmacol.* **70,** 1575–1584
48. Wisler, J. W., DeWire, S. M., Whalen, E. J., Violin, J. D., Drake, M. T., Ahn, S., Shenoy, S. K., and Lefkowitz, R. J. (2007) A unique mechanism of β-blocker action. Carvedilol stimulates β-arrestin signaling. *Proc. Natl. Acad. Sci. U.S.A.* **104,** 16657–16662
49. Rajagopal, S., Rajagopal, K., and Lefkowitz, R. J. (2010) Teaching old receptors new tricks: biasing seven-transmembrane receptors. *Nat. Rev. Drug Discov.* **9,** 373–386
50. Jensen, B. C., Swigart, P. M., and Simpson, P. C. (2009) Ten commercial antibodies for α-1-adrenergic receptor subtypes are nonspecific. *Naunyn Schmiedebergs Arch. Pharmacol.* **379,** 409–412
51. Bulenger, S., Marullo, S., and Bouvier, M. (2005) Emerging role of homo- and heterodimerization in G-protein-coupled receptor biosynthesis and maturation. *Trends Pharmacol. Sci.* **26,** 131–137
52. Milligan, G. (2008) A day in the life of a G protein-coupled receptor. The contribution to function of G protein-coupled receptor dimerization. *Br. J. Pharmacol.* **153,** S216–S229
53. Lohse, M. J. (2010) Dimerization in GPCR mobility and signaling. *Curr. Opin. Pharmacol.* **10,** 53–58
54. Hern, J. A., Baig, A. H., Mashanov, G. I., Birdsall, B., Corrie, J. E., Lazareno, S., Molloy, J. E., and Birdsall, N. J. (2010) Formation and dissociation of M1 muscarinic receptor dimers seen by total internal reflection fluorescence imaging of single molecules. *Proc. Natl. Acad. Sci. U.S.A.* **107,** 2693–2698
55. Schelshorn, D., Joly, F., Mutel, S., Hampe, C., Breton, B., Mutel, V., and Lütjens, R. (2012) Lateral allosterism in the glucagon receptor family. Glucagon-like peptide 1 induces G-protein-coupled receptor heteromer formation. *Mol. Pharmacol.* **81,** 309–318
56. Rovira, X., Pin, J. P., and Giraldo, J. (2010) The asymmetric/symmetric activation of GPCR dimers as a possible mechanistic rationale for multiple signaling pathways. *Trends Pharmacol. Sci.* **31,** 15–21
57. Maurice, P., Kamal, M., and Jockers, R. (2011) Asymmetry of GPCR oligomers supports their functional relevance. *Trends Pharmacol. Sci.* **32,** 514–520
58. Pfleger, K. D., and Eidne, K. A. (2006) Illuminating insights into protein-protein interactions using bioluminescence resonance energy transfer (BRET). *Nat. Methods* **3,** 165–174
59. Oakley, R. H., Laporte, S. A., Holt, J. A., Barak, L. S., and Caron, M. G. (1999) Association of β-arrestin with G protein-coupled receptors during clathrin-mediated endocytosis dictates the profile of receptor resensitization. *J. Biol. Chem.* **274,** 32248–32257
60. Oakley, R. H., Laporte, S. A., Holt, J. A., Barak, L. S., and Caron, M. G. (2001) Molecular determinants underlying the formation of stable intracellular G protein-coupled receptor-β-arrestin complexes after receptor endocytosis. *J. Biol. Chem.* **276,** 19452–19460
61. Vázquez-Prado, J., Medina, L. C., Romero-Avila, M. T., González-Espinosa, C., and García-Sáinz, J. A. (2000) Norepinephrine- and phorbol ester-induced phosphorylation of α(1a)-adrenergic receptors. Functional aspects. *J. Biol. Chem.* **275,** 6553–6559
62. Tobin, A. B., Butcher, A. J., and Kong, K. C. (2008) Location, location, location . . . site-specific GPCR phosphorylation offers a mechanism for cell-type-specific signalling. *Trends Pharmacol. Sci.* **29,** 413–420
63. Butcher, A. J., Prihandoko, R., Kong, K. C., McWilliams, P., Edwards, J. M., Bottrill, A., Mistry, S., and Tobin, A. B. (2011) Differential G-protein-coupled receptor phosphorylation provides evidence for a signaling bar code. *J. Biol. Chem.* **286,** 11506–11518
64. Nobles, K. N., Xiao, K., Ahn, S., Shukla, A. K., Lam, C. M., Rajagopal, S., Strachan, R. T., Huang, T. Y., Bressler, E. A., Hara, M. R., Shenoy, S. K., Gygi, S. P., and Lefkowitz, R. J. (2011) Distinct phosphorylation sites on the β2-adrenergic receptor establish a barcode that encodes differential functions of β-arrestin. *Sci. Signal.* **4,** ra51
65. Liggett, S. B. (2011) Phosphorylation barcoding as a mechanism of directing GPCR signaling. *Sci. Signal.* **4,** pe36
66. Thorsteinsson, A., Johannesdottir, A., Eiríksson, H., and Helgason, H. (2008) Severe labetalol overdose in an 8-month-old infant. *Paediatr. Anaesth.* **18,** 435–438
67. Dalrymple, M. B., Jaeger, W. C., Eidne, K. A., and Pfleger, K. D. (2011) Temporal profiling of orexin receptor-arrestin-ubiquitin complexes reveals differences between receptor subtypes. *J. Biol. Chem.* **286,** 16726–16733